ISSN 2063-5346

ENGINEERING NANOTEXTURED TITANIUM SURFACES

*Sachin M. Bhosle [1], Craig R. Friedrich [2]

[1, 2] Department of Mechanical Engineering, Multi-Scale Technologies Institute, Michigan Technological University, Houghton, MI, USA
[1] Department of Mechanical Engineering, Vidya Pratishthan's Kamalnayan Bajaj Institute of Engineering and Technology, Baramati, MH, India
[1]smbhosle@mtu.edu

Article History: Received: 01.10.2022 **Revised:** 22.11.2022 **Accepted:** 24.12.2022

Abstract
Nanotextured titanium oxide surfaces were obtained by electrochemical anodization of Ti6Al4V alloy. Two different types of electrolytes containing different amounts of water and NH4F concentration in ethylene glycol were used. This work focused on structural modifications by varying the F- ion concentration in the electrolyte, anodization voltage and time. The effect of these anodization parameters on nanotextured morphology and dimensions was studied. The titania nanotube diameters ranging from 50 to 135 nm, and the lengths ranging from 0.5 to 5 µm, were obtained. The morphology showed strong dependence on electrolyte composition whereas, the nanotube dimensions showed dependence on anodization voltage and time. To extend the possibility of fabricating nanotubes on a wide range of Ti6Al4V implant surfaces such as rolled surfaces, thermal plasma sprayed surfaces, and next generation orthopedic implant surfaces made by powder metallurgy, were also targeted in this study.
Key words: orthopedic; TiO_2 nanotube, electrochemical anodization, surface modification.

1. Introduction

The corrosion resistance, superior mechanical properties and good biocompatibility makes titanium and its alloys favorable candidate for implant materials [1]. The nanophase materials on orthopedic implants have been suggested to improve bonding between an implant and surrounding bone with aid in bone cell functions [2]. The oxide layer formed by electrochemical anodization has shown improved biocompatibility of titanium implants [3]. In biomedical applications, the control of morphology, dimensions and phase composition plays a vital role in determining the effectiveness of the modified implant surface. A TiO_2 nanotube (TiNT) layer fabricated on implant surfaces by electrochemical anodization enhances osseointegration and stability [4,5]. Zwilling and co-workers reported self-organized anodic nanotube layer of titanium oxide for the first time in 1999, recognizing that the fluorine ions in the electrolyte are responsible for tube formation and the tubular structure formed was amorphous [6]. Gong et al. reported fabrication of TiNTs by electrochemical anodization using hydrofluoric acid based electrolyte with diameters of nanotubes

ranging from 25 – 65nm [7]. Electrochemical anodization produces a layer of nanotubes open at the top and closed at the bottom whose diameter and length can be controlled by using appropriate electrolyte concentration, anodization voltage and time. Over the years several research groups have focused on nanotube synthesis using electrochemical anodization with different nanotube diameters ranging from 65 nm to 150 nm and lengths ranging from 250 nm to 134 μm [7-12]. The nanoscale dimensions can change the ionic, electronic and bio-interface properties considerably, which may help to improve reaction/interaction between an implant and the surrounding tissue [13]. Anodization parameters influence nanotube formation causing morphological variations in their length, diameter, wall thickness and inter-tubular spacing. This calls for better understanding of the influential factors governing the self-organization and dimensions of titania nanotubes during the anodization process, focusing on the specific type of electrolyte and anodization conditions from a wide range. Our implant surface modification technology is based on safe, low-cost electrochemical fabrication of nanotextured surfaces on implants. This process uses relatively nonhazardous materials (NH_4F instead of hydrofluoric acid), is environmentally safe and requires minimal maintenance. The objective of the present study was to quantify the effect of electrolyte composition on nanotube morphology and the effect of anodization voltage and time on nanotube dimensions on test materials and commercial implants. To investigate the effect of electrolyte composition on nanotube morphology, two different electrolyte compositions, with different fluorine concentration and deionized water in ethylene glycol were used. To extend the fabrication of nanotubular surfaces over a wide range of Ti6Al4V alloy substrates, rolled rods, Kirschner wires (K-wires), thermal plasma sprayed surfaces (TPS) and powder metallurgically (PM) manufactured (laser-sintered and electron-beam sintered) porous cylinders, were studied in this work. Suitable electrochemical anodization recipes to successfully fabricate a nanotube layer on these surfaces was determined and the morphological and chemical nature of the resulting surfaces was studied. The purpose of this work was to provide a set of fabrication guidelines to design a process for a specified implant surface morphology.

2 Materials and Methods

2.2.1 Substrate preparation

Foils (12mm x 12mm x 0.5mm thick) ASTM B 265-11 grade 5 (TIMET, USA), rods (3mm diameter), K-wires (1mm diameter), thermal plasma sprayed (24mm diameter and 12mm long) commercial implant sections of Ti6Al4V alpha/beta titanium alloy were cleaned in deionized (DI) water followed by acetone and dried in air at room temperature. Additionally, two types of powder metallurgically (PM) manufactured porous cylinder implants (8mm diameter x 20mm long) of Ti6Al4V, electron beam sintered (ArCam, USA) and laser-sintered (DMLS, USA) were cleaned ultrasonically in DI water only and dried in air at room temperature.

2.2.2 Fabricating nanotubes

The nanotextured porous surfaces were fabricated by electrochemical anodization using a DC power source (Protek 3006B), with direct current (DC) output 0-60V, 1.5A as shown in Fig.2.1. The surfaces were anodized at room temperature with a graphite rod as the cathode and the titanium alloy as the anode. Two electrolyte recipes used to anodize the nanotubes with specific compositions, as listed in Table 2.1, are hereafter abbreviated LWHF (low-water, high-fluorine) and HWLF (high-water, low-fluorine).

Table 2.1 Anodization conditions used for fabrication of TiNT surfaces

Receipe	Electrolyte solution	Potential (V)	Anodization time
LWHF	98% EG + 2% DI water + 0.6 wt% NH_4F	30 - 60	25 to 40 minutes
HWLF	60% EG + 40% DI water + 0.2 wt% NH_4F	30	1 to 4 h

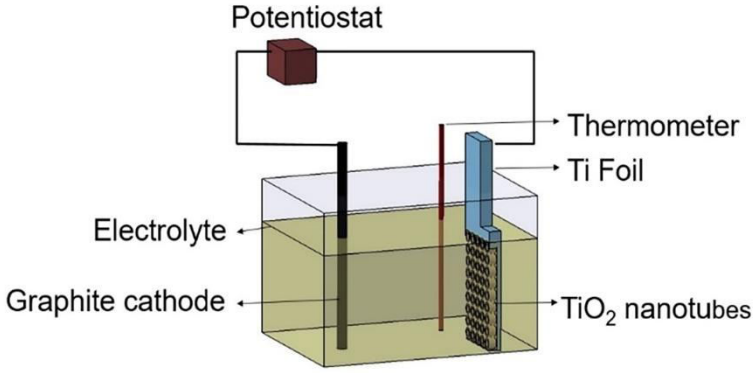

Figure 2.1 Electrochemical anodization setup for fabrication of TiO_2 nanotube surface. The nanotube can be etched on variety of substrates shown in setup as Ti foil.

2.2.3 Surface characterization

Characterization of the anodized surfaces was performed by field emission scanning electron microscopy (FE-SEM, Hitachi S-4700). The wt% chemical compositional analysis of surfaces was by energy dispersive spectroscopy (EDS) with standardless quantitative analysis on the FESEM at 10kV.

3 Results and Discussion

3.3.1 Effect of electrolyte recipe on morphology

Electrochemical anodization using two different electrolytes resulted in formation of two different TiNT morphologies (Fig.3.2). Each type of TiNT structure showed a strong dependence on electrolyte composition. The nanotubes formed in the LWHF electrolyte at 60V for 40 minutes produced a honeycomb-like, tightly bound, vertically aligned structure with smooth nanotube walls (Fig.3.2b). These tubes present an ordered and well packed structure (Fig.3.2a). In contrast, the nanotubes formed in the HWLF electrolyte at 30V for 4h produced well-spaced, individual-vertically aligned structures (Fig.3.2c). These nanotubes showed ripples in their side walls (Fig.3.2d).

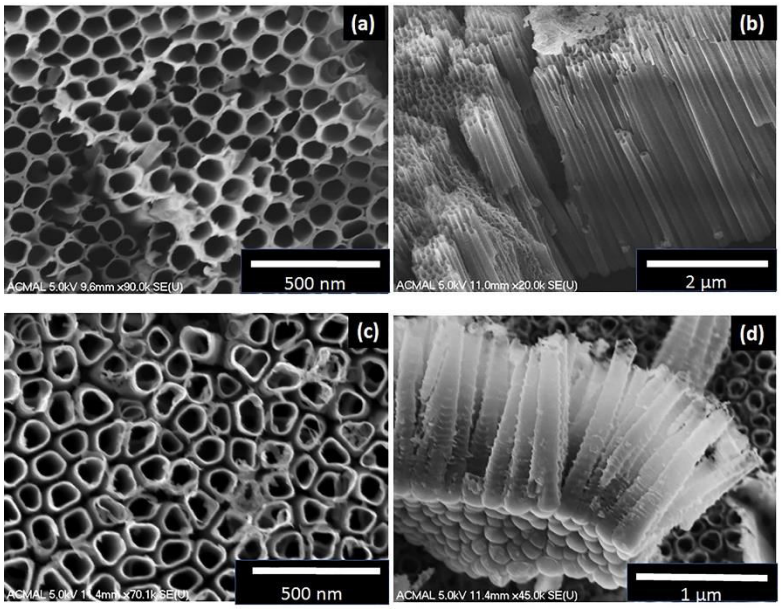

Figure 3.2 Nanotube morphologies obtained with (a-b) LWHF and (c-d) HWLF electrolytes.

3.3.2 Rib formation on tube walls

The major difference observed between the two types of morphologies was the presence of ribs on the external walls of the nanotubes obtained with HWLF electrolyte. The electrochemical oxidation of titanium and subsequent dissolution of oxide by fluoride ions leads to the formation of TiF_6 complexes per the reactions: [14].

$$Ti + 2H_2O \rightarrow TiO_2 + 4H^+ + 4e^-$$

$$TiO_2 + 4H^+ + 6F^- \rightarrow [TiF_6]^{2-} + 2H_2O$$

The rib formation on the tube walls occurs as a result of partial dissolution of $[TiF_6]^{2-}$ complexes between cell boundaries while simultaneous oxide dissolution continues leading to deepening of the main tubes during anodization. The barrier layer formed between adjacent tubes due to partially dissolved complexes, facilitates migration of cations (F^-, O^{2-}) and anions (Ti^{4+}). This leads to film formation (comprised of oxide and fluorine rich complexes) at the nanotube boundaries. Upon dissolution of the fluorine rich metal complexes, the oxide-rich portion results in the formation of ribs on nanotube walls [15].

3.3.3 Effect of voltage with LWHF electrolyte

To study the effect of anodization voltage on nanotube size, the titania nanotube layers were obtained over a range of anodization voltage. The anodization process was carried out for 40 minutes at 30, 40, 50 and 60V in LWHF electrolyte. Fig.3.3. shows the FESEM micrographs of nanotube diameters and lengths. The relationship between anodization voltage (V) and outer nanotube diameter (D) is summarized in Fig.3.4a. The outer diameter of nanotubes ranged from 50±2.5 nm to 100±3nm for anodization voltages from 30 to 60V. Fig.3.4b summarizes the relationship between anodization voltage and nanotube length (L). For 30, 40, 50 and 60V an average length of 1.5, 2.8, 3.9 and 4.7 microns was observed. The bars show the standard deviations of repeated measurements. It was evident that the outer diameter and length increases with anodization voltage and the relationship can be linearized per Eq. (1) for diameter, and Eq. (2) for length, over the specified range of voltage between 30 to 60V.

$$D = 1.4V+12 \quad (1)$$

$$L = 0.1V–1.66 \quad (2)$$

This linear relationship can be ascribed to the fact that the thickness of the anodic oxide film linearly increases with the voltage in forming a compact oxide during

the initial stage of tube growth [14]. At higher anodization voltage, larger anodic current during nanotube formation produces longer length of tubes [16]. It is recognized that Eq. (1) and (2) prescribe nanotubes with zero voltage, however the constants are necessary over the 30V-60V range.

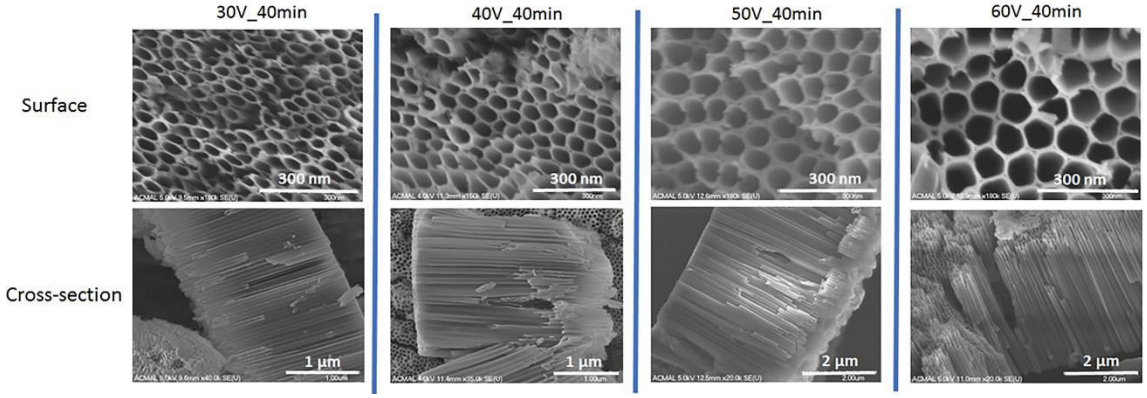

Figure 3.3 Nanotube morphologies obtained with LWHF electrolyte by varying anodization voltage.

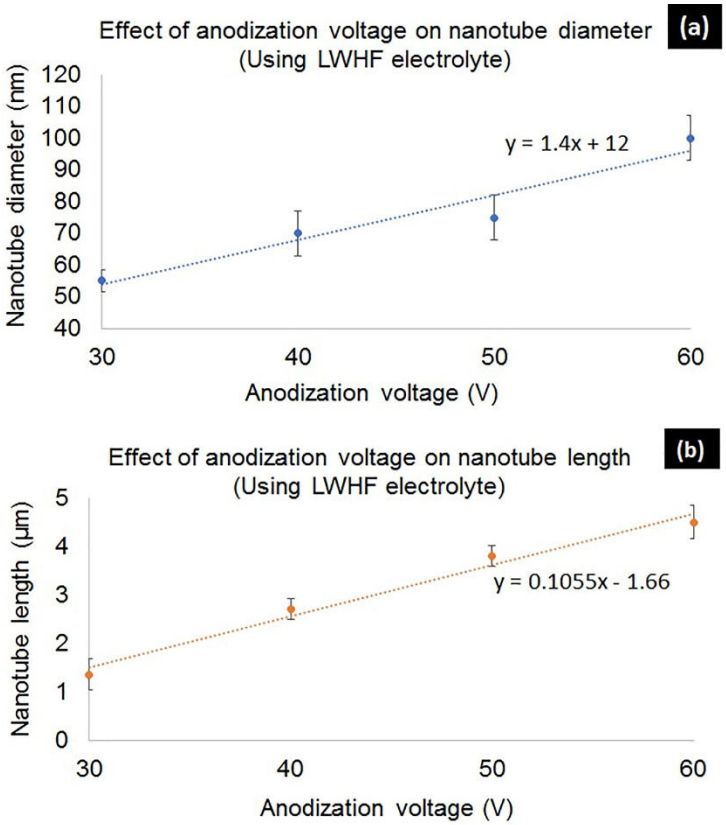

Figure 3.4 Effect of anodization voltage on tube diameter (a) and length (b) using LWHF electrolyte.

3.3.4 Effect of anodization time with LWHF electrolyte

To study the effect of anodization time on nanotube size, another set of experiments was conducted at constant voltage and varying time. The anodization process was at 60V for 25, 30, 35 and 40 minutes. Fig.3.5 shows the FESEM micrographs of nanotube diameters and lengths obtained over the selected range of anodization time. Fig.3.6a summarizes the relationship between anodization time and outer

nanotube diameter. For 25, 30, 35 and 40-minute anodization at 60V, the average diameters of 80, 82.5, 82.5 and 95 nm were observed. This variation in nanotube diameter was much less than variation observed with change in anodization voltage indicating that voltage is a stronger factor for diameter than is time. Fig.3.6b summarizes the relationship between anodization time and nanotube length. For 25, 30, 35 and 40-minute anodization at 60V, the average nanotube length of 3.8, 4, 4.3 and 4.7 microns were observed. Again, this variation in nanotube length is much less than the variation observed with changes in voltage. Thus, the anodization voltage has shown more influence on tube dimensions than anodization time.

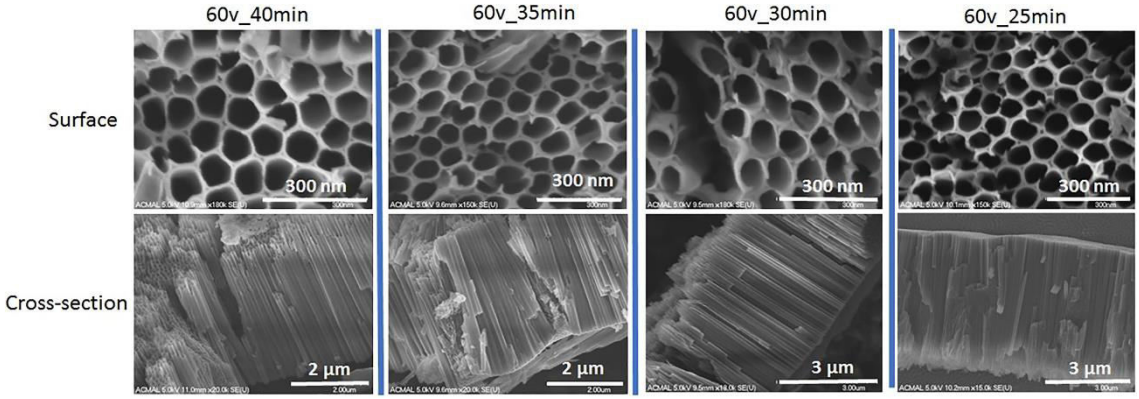

Figure 3.5 Nanotube morphologies obtained with LWHF electrolyte by varying anodization time.

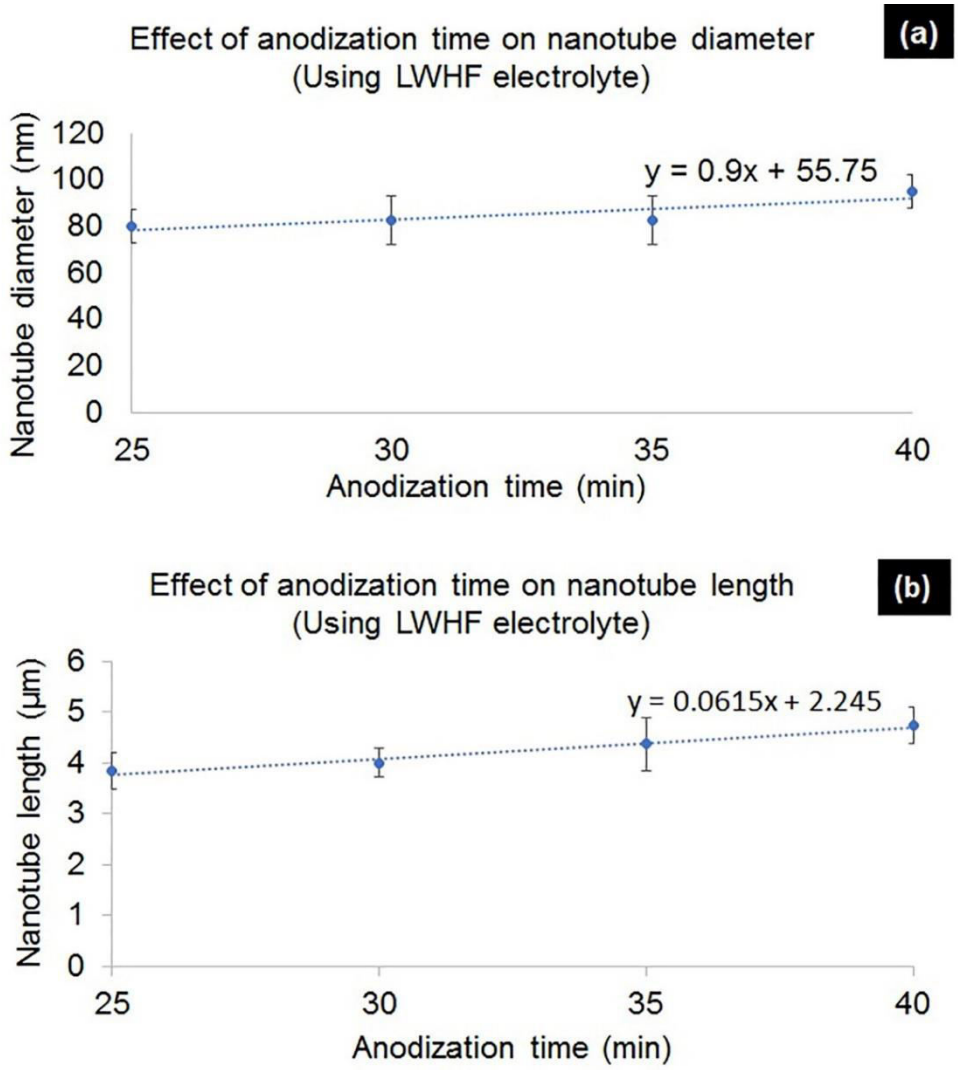

Figure 3.6 Effect of anodization time on tube diameter (a) and length (b) using LWHF electrolyte.

3.3.5 Effect of anodization time with HWLF electrolyte

The effect of variation in anodization time (at 30V) on tube length and diameter using HWLF is shown by FESEM micrographs in Fig.3.7. The relationship between anodization time and outer nanotube diameter is summarized in Fig.3.8a. For 1, 2, 3 and 4h anodization at 30V, the average diameter of 97, 122, 117 and 122 nm were observed. Fig. 3.8b summarizes the relationship between anodization time and nanotube length. For 1, 2, 3 and 4 h anodization at 30V, the average length of 0.5, 0.7, 1.1 and 1.25 micron were observed.

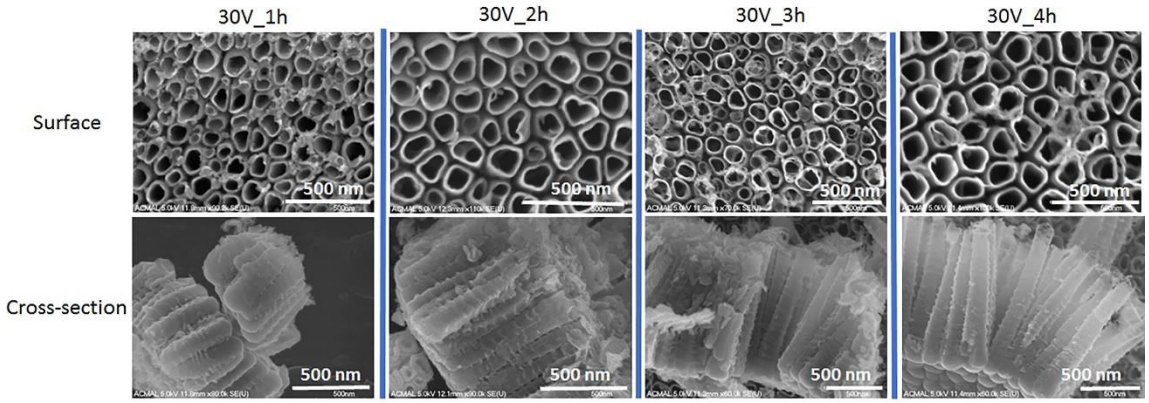

Figure 3.7 Nanotube morphologies obtained with HWLF electrolyte by varying anodization time.

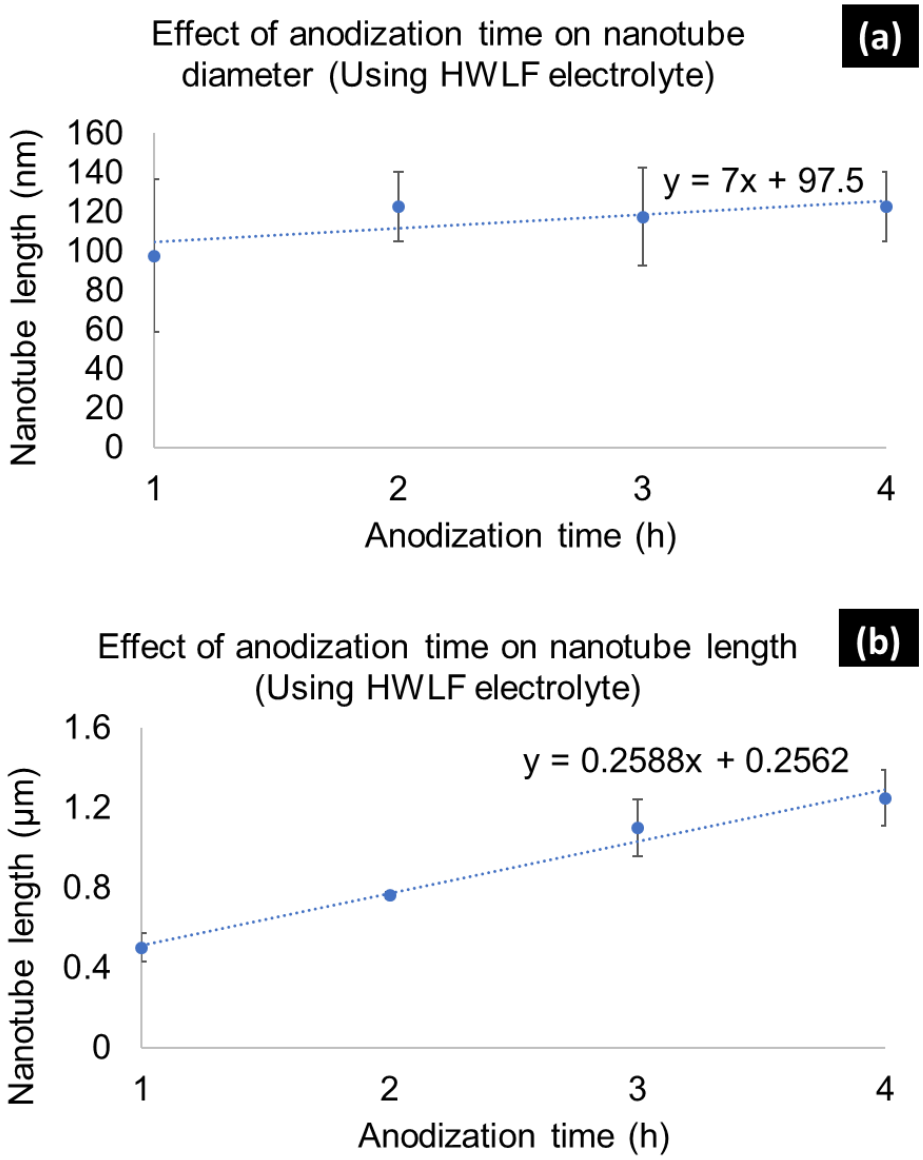

Figure 3.8 Effect of anodization time on tube diameter (a) and length (b) using HWLF recipe.

3.3.6 Effect of electrical conductivity of electrolyte on TiNT morphology

It is reported that, upon reuse of electrolyte, the metal contaminants dissolved during anodization decreases the electrical conductivity of the electrolyte and subsequent current densities lead to change in resulting morphology [17]. The anodization by-products released into the electrolyte are particles of various oxides of titanium, aluminium and vanadium. As this increase in concentration in the electrolyte, the conductivity decreases. Also as fluorine is depleted in the electrolyte, the conductivity further decreases due to reduced ionic strength. The resulting nanostructure morphology also depends on the electrical conductivity of the electrolyte and fluoride ion concentration. To investigate the more influential factor among these two, additional experiments were conducted. To investigate the effect of decreased electrical conductivity due to metals contamination, resistances ranging from 300 Ω to 33 kΩ were added in series. LWHF electrolyte containing 0.6 wt% NH_4F was used for anodization of titanium alloy foils to study the influence of resistances in series (simulated decrease of electrical conductivity of electrolyte) on resulting morphology. Fig.3.9 shows the effect of decreased electrical conductivity of the electrolyte on resulting morphology upon anodization. Only pits and pores of 10 – 20 nm were formed and no tubes were observed with 8.2 kΩ and 33 kΩ resistance. Tube formation initiated with 3.9 kΩ resistance and tube diameters of 50nm was observed. Well defined, self-ordered tubular structures were observed with 1.8 kΩ and 300 Ω resistances. The tube diameters of 65 nm and 85 nm were observed with 1.8 kΩ and 300 Ω resistance, respectively. Although the variation in tube diameter was observed, this indicates that there was sufficient fluorine ion concentration in the electrolyte to provide enough electrical conductivity required for formation of tubular morphology. This also indicates that fluorine concentration in the electrolyte is the more dominating parameter affecting electrical conductivity of the electrolyte. Thus, as resistance in series was decreased, the increased current density led to formation of tubular structures. From a biological perspective, if nanoporous structures, instead of tubular structures are required, this process can fabricate nanoporous structures of required sizes without changing the electrolyte just by putting appropriate resistance in series.

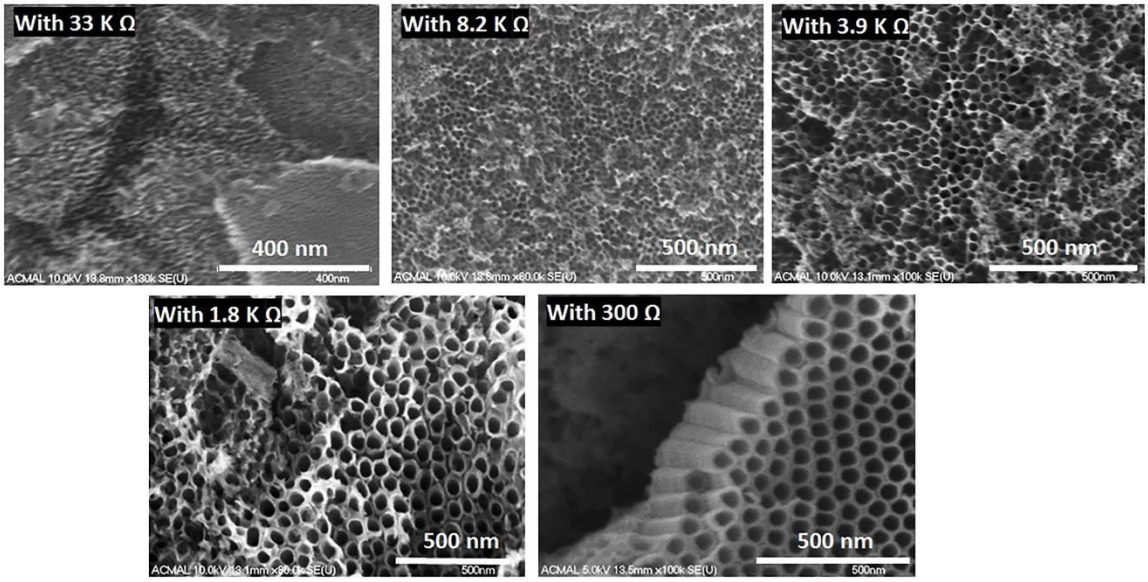

Figure 3.9 Effect of electrical resistances in series on morphology.

3.3.7 Effect of fluoride concentration in electrolyte

To investigate the influence of F^- ion concentration on the electrical conductivity of the electrolyte and resulting morphology, another set of experiments was conducted. LWHF electrolyte containing 2 vol% of DI water with varying concentration of NH_4F was used. FESEM micrographs in Fig.3.10 show the effects of varying F^- ion concentration in the electrolyte on anodized surface morphology. For 0.1 and 0.3 wt% NH_4F, only pores of diameter approximately 25 nm and 80 nm were observed respectively. Whereas using 0.66 wt% NH_4F, the formation of tubular morphology with 100 nm tube diameter was observed. Thus, among two factors viz. resistances in series simulating metals contamination in the electrolyte and varying F^- concentration in the electrolyte causing a decrease in electrical conductivity and current transients during anodization, the F^- concentration was observed to be the more influential factor affecting formation of porous or tubular structures.

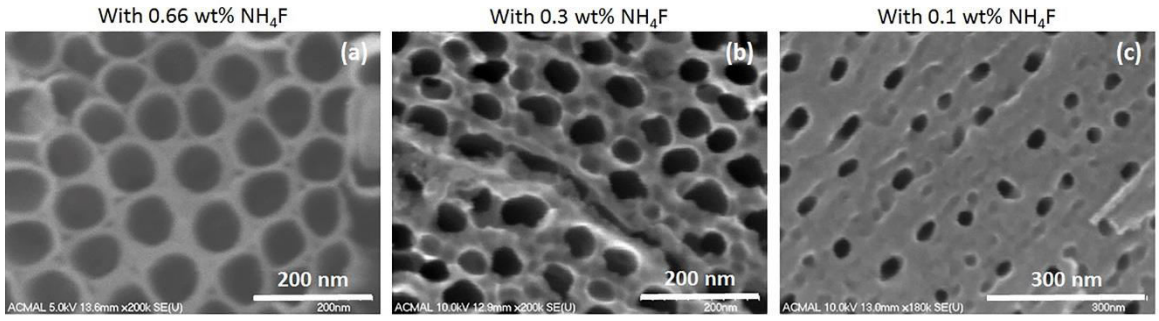

Figure 3.10 Effect of F^- ion concentration in electrolyte on morphology. Resulting structure using 0.6 wt% (a); 0.3 wt% (b); and 0.1 wt% (c); NH_4F in electrolyte solution.

3.3.8 Nanotubes fabricated on powder metallurgically made implants

The porous surfaces made by powder metallurgy (laser-sintered and electron-beam sintered) were anodized using HWLF electrolyte. Anodization voltage and time were varied in two different sets of experiments to obtain the processing conditions for the desired nanotube structure. The laser-sintered surfaces were

anodized at 60V for 40 minutes in HWLF electrolyte. The tube diameter observed was 100 ± 10 nm and tube length was 500 nm (Fig.3.11). No nanotube morphologies were detected at 60V after 40 min anodization on electron-beam sintered surfaces (not shown here). Therefore, the electron beam- sintered surfaces were anodized at 30V for 4h. The tube diameter of 90 ± 10 nm and tube length of 450 ± 20 nm were observed (Fig.3.12). In both cases, tubes were observed on all powder particles and other surfaces to which powder particles were attached.

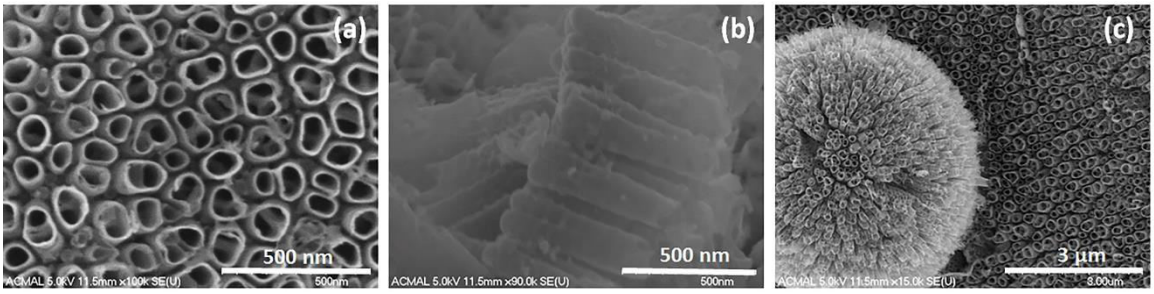

Figure 3.11 FESEM micrographs of nanotube surface formed on powder metallurgically manufactured laser-sintered Ti alloy surface with HWLF at 60V for 40 min. (a) top view of surface; (b) cross-section of nanotube layer; (c) nanotube morphology obtained on powder particles and underneath surface. (Samples were provided courtesy of Nanovation Partners, LLC).

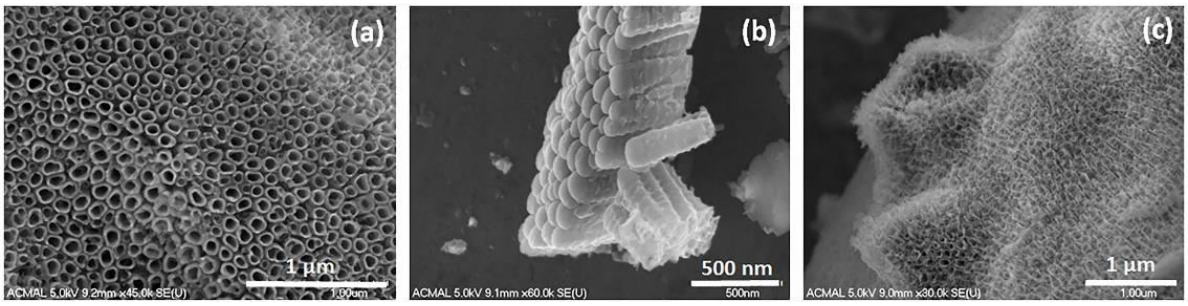

Figure 3.12 Nanotube surface formed on powder metallurgically manufactured electron beam-sintered Ti alloy surface with HWLF at 30V for 4h. (a) top view of surface; (b) cross-section of nanotube layer; (c) nanotube morphology obtained on powder particles and underneath surface. (Samples were provided courtesy of Nanovation Partners, LLC).

3.3.9 Chemistry of TiO_2 nanotubes fabricated on PM porous cylinders

The energy-dispersive X-ray spectroscopy (EDS) results summarized in Table 3.2 indicated the chemical composition of TiNT surfaces fabricated on powder metallurgically manufactured porous cylinders of Ti6Al4V. Residual fluorine of 3.79 and 4.51 wt% was observed in the laser-sintered and electron beam sintered surfaces. The possible source of nitrogen detected could be NH_4F added to make the electrolyte and carbon is detected from carbon tape used mounting the samples for FESEM-EDS examination. Because these materials were formed at high temperature, the chemistry may have changed from the initial alloy powder chemistry, with the possible addition of carbon.

Table 3.2 Comparison of chemical composition of TiNT surfaces on powder metallurgically manufactured titanium alloy surfaces.

Type of surface and anodization conditions	Relative wt% of elements						
	Ti	Al	V	O	F	C	N
Laser-Sintered (60V_40min)	60.76	5.35	1.58	23.41	3.79	0.15	4.97
E-beam Sintered (30V_4h)	56.97	5.54	1.09	26.32	4.51	0.63	4.94

3.3.10 Nanotubes fabricated on thermal plasma sprayed (TPS) titanium alloy surfaces

In vivo studies of thermal plasma sprayed (TPS) implants are reported to show increased bone contact and accelerated bone formation [18]. TPS alloy implant pieces were electrochemically anodized in HWLF electrolyte with two different anodization conditions on different implants to analyze nanotube morphology. Fig.3.13a shows a TiNT surface fabricated at 30V for 4h. The porous surface with an average pore size of 25-30nm was observed. Fig.3.13b shows a TiNT surface fabricated at 60V for 40 minutes. It is evident that the nanotubes were anodized on the entire surface covering all the macroscopic roughness features. Nanotube diameters of 35-40nm and lengths of 500nm were observed with 60V in 40min anodization. The TiNTs on the TPS alloy substrate were vertically oriented, laterally spaced and structurally stable. This porous network of nanotubes showed strong scratch resistance representing good mechanical strength needed to sustain surgical loads

.

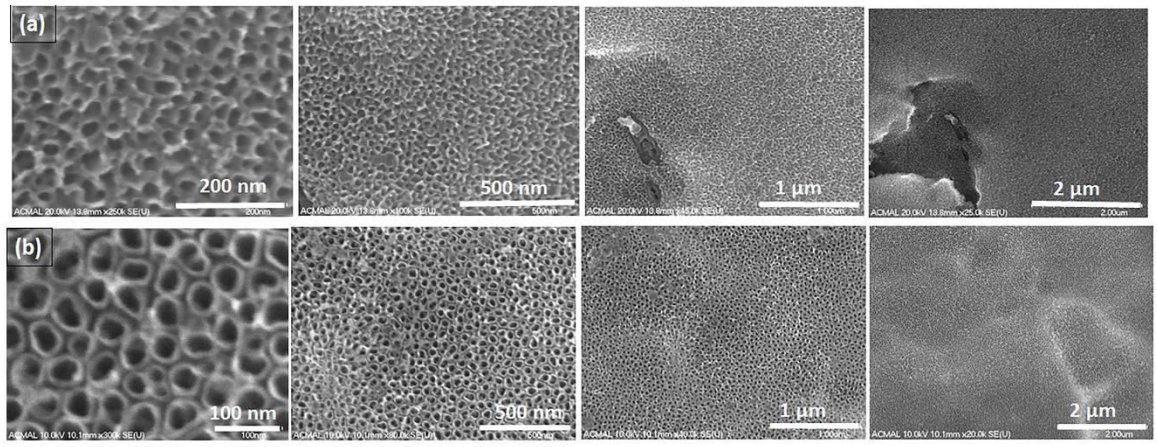

Figure 3.13 FESEM micrographs of nanotube surface formed on TPS titanium alloy with HWLF (a) at 30V in 4h; (b) at 60V in 40min.

3.3.11 Chemistry of TiO_2 nanotubes fabricated on TPS titanium alloy

The energy-dispersive spectroscopy results summarized in Table 3.3 indicated the chemical composition of TiNT surfaces fabricated on TPS Ti6Al4V. Residual fluorine of about 6.25 wt% was observed in nanotube surfaces anodized at 60V in 40 min. This residual fluorine was released upon annealing. In these, and all anodized surfaces, there is a large increase in oxygen indicating the formation of TiO_2 which is the biocompatible layer for titanium implants.

Table 3.3 Chemical composition of as-received and anodized TiNT on TPS titanium alloy surfaces

Type of surface and condition	Relative wt% of elements				
	Ti	Al	V	O	F
As-received TPS	89.04	8.88	2.07	--	--
Nanotube layer anodized on TPS at 60V in 40min	62.45	5.73	3.52	22.05	6.25

3.3.12 Nanotubes fabricated on K-wires

TiNT structures were fabricated on 1mm diameter K-wires of Ti6Al4V using LWHF electrolyte. These were used as femur implants in rats to study the influence of TiNT structure on bone formation and bone-implant stability via *in vitro* experiments as well as an *in vivo* model of femoral intramedullary fixation [19]. It has been demonstrated that osteogenic functions of cultured cells were improved on TiNT surfaces compared to as-received surfaces *in vitro* whereas, increased bone formation on TiNT surfaces was observed *in vivo*. Fig.3.14 shows as received and TiNT morphology achieved with anodization at 60V for 40 min. Tube diameters of 100 nm and length of 1 µm were observed. The chemical composition of as-received and the anodized TiNT surfaces fabricated on K-wires are summarized in Table 3.4. Residual fluorine of about 8.46 wt% was observed in the nanotube surface. Table 3.5. summarizes the surface properties and anodization conditions for different Ti6Al4V substrates.

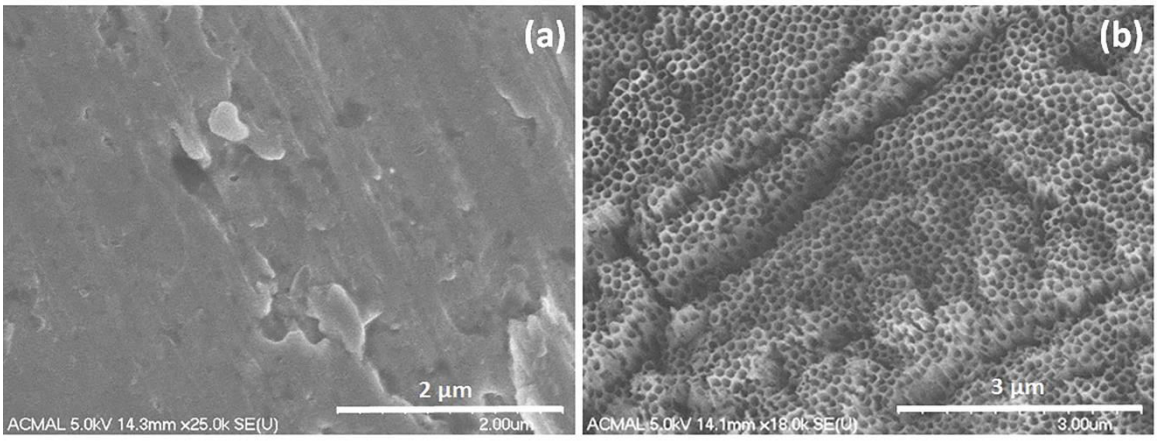

Figure 3.14 Micrographs of K-wires (a) as-received surface; (b) anodized in LWHF at 60V for 40 min showing nanotubes.

Table 3.4 Chemical composition of as-received and anodized TiNT on titanium alloy K-wires

Type of surface and condition	Relative wt% of elements				
	Ti	Al	V	O	F
As-received	89.6	7.13	3.05	0.21	0
TiNT layer anodized at 60V in 40min	58.26	3.81	1.76	27.7	8.46

Table 3.5 Surface properties and anodization conditions for different Ti6Al4V substrates.

Alloy substrate	Electrolyte	Anodization voltage	Anodization time	Tube diameter (nm)	Tube Length (µm)

Foil	LWHF	60V	40min	90 ± 10	4.5
Rod	LWHF	60V	40min	95 ± 5	4.7
Rod	HWLF	30V	4h	122	1.25
K-wire	LWHF	60V	40min	100	1
TPS	HWLF	60V	40min	35 - 40	0.5
TPS	HWLF	30V	4h	25 – 30	--
Laser-sintered PM part	HWLF	60V	40min	100 ± 10	0.5
Electron-beam sintered PM part	HWLF	30V	4h	90 ± 20	0.45

4 Conclusions

The present work showed that nanotextured morphology depends on electrolyte composition, and dimensional variation depends on anodization conditions on Ti6Al4V alloy surfaces using different NH_4F and ethylene glycol electrolytes. It was observed that different surfaces of Ti6Al4V need different electrolyte composition and anodization conditions to get nanotubes. This work will help to control morphology and dimensions of titanium oxide nanotubes for potential applications in biomedical implant applications. The much longer tube length of about 4.7 microns obtained in 40 minutes using LWHF electrolyte, compared to 1.25 micron obtained in 4h using HWLF, demonstrates a much more aggressive oxide dissolution rate with higher fluorine concentration in the electrolyte and higher anodization voltage. Resistances in series (simulating metals contamination) and varying F^- concentration in electrolyte caused a decrease in electrical conductivity and current transients during anodization. The F^- concentration was found to be the most influential factor affecting formation of porous nanostructures. This also showed that by inserting resistance in the anodization circuit, porous structures can be formed with the same electrolyte further demonstrating the versatility of this process. It was also shown that commercial TPS, and laser-sintered and electron-beam melted powder implants are easily processed to create nanotube surfaces.

References

[1] Niiomi M. Recent Metallic Materials for Biomedical Applications. Metallurgical and Materials Transactions A. 2002;33A:477-86.

[2] Balasundarama G, Webster TJ. A perspective on nanophase materials for orthopedic implant applications. Journal of Materials Chemistry. 2006;16:3737–45.

[3] Lausmaa J. Surface spectroscopic characterization of titanium implant materials. Journal of Electron Spectroscopy and Related Phenomena. 1996;81:343-61.

[4] Oh S, Daraio C, Chen LH, Pisanic TR, Finones RR, Jin S. Significantly accelerated osteoblast cell growth on aligned TiO_2 nanotubes. J Biomed Mater Res A. 2006;78:97-103.

[5] Jang I, Shim SC, Choi DS, Cha BK, Lee JK, Choe BH, et al. Effect of TiO_2 nanotubes arrays on osseointegration of orthodontic miniscrew. Biomed Microdevices. 2015;17:76.

[6] Zwilling V, Darque-Ceretti E, Boutry-Forveille A, David D, Y. PM, M. A. Structure and Physicochemistry of Anodic OxideFilms on Titanium and TA6V Alloy. Surface and Interface Analysis. 1999;27:629-37.

[7] Gong D, Grimes CA, OOmman KV, Wenchong H, Singh RS, Chen Z, et al. Titanium oxide nanotube arrays prepared by anodic oxidation. Journal of Materials Research. 2001;16:3331-34.

[8] Cai Q, Paulose M, Varghese OK, Grimes CA. The effect of electrolyte composition on the fabrication of self-

organized titanium oxide nanotube arrays by anodic oxidation. Journal of Materials Research. 2011;20:230-6.
[9] Xiao X, Ouyang K, Liu R, Liang J. Anatase type titania nanotube arrays direct fabricated by anodization without annealing. Applied Surface Science. 2009;255:3659-63.
[10] Lai YK, Sun L, Chen C, Nie CG, Zuo J, Lin CJ. Optical and electrical characterization of TiO_2 nanotube arrays on titanium substrate. Applied Surface Science. 2005;252:1101-6.
[11] Paulose M, Grimes CA. Anodic Growth of Highly Ordered TiO_2 Nanotube Arrays to 134 μm in Length. Journal of Physical Chemistry Letters B. 2006;110:16179-82.
[12] Friedrich CR, Shokuhfar T. Compositions methods and devices for generating nanotubes on a surface. United States Patent US 20130196128. 2016.
[13] Roy P, Berger S, Schmuki P. TiO_2 nanotubes: synthesis and applications. Angewandte Chemie International Edition Engl. 2011;50:2904-39.
[14] Yasuda K, Schmuki P. Control of morphology and composition of self-organized zirconium titanate nanotubes formed in $(NH_4)_2SO_4/NH_4F$ electrolytes. Electrochimica Acta. 2007;52:4053-61.
[15] Valota A, LeClere DJ, Skeldon P, Curioni M, Hashimoto T, Berger S, et al. Influence of water content on nanotubular anodic titania formed in fluoride/glycerol electrolytes. Electrochimica Acta. 2009;54:4321-7.
[16] Yasuda K, Schmuki P. Formation of Self-Organized Zirconium Titanate Nanotube Layers by Alloy Anodization. Advanced Materials. 2007;19:1757-60.
[17] Bhosle SM, Tewari R, Friedrich CR. Dependence of nanotextured titanium orthopedic surfaces on electrolyte condition. Journal of Surface Engineered Materials and Advanced Technology. 2016;06:164-75.
[18] Darimont GL, Cloots R, Heinen E, Seidel L, Legrand R. In vivo behaviour of hydroxyapatite coatings on titanium implants: a quantitative study in the rabbit. Biomaterials. 2002;23:2569-75.
[19] Vara A, Baker EA, Salisbury M, Fleischer M, Bhosle SM, Friedrich C, et al. Enhancing osseointegration of orthopaedic implants with titania nanotube surfaces. Foot & Ankle Orthopaedics. 2016;1:1.